Chapter 5

Role of Band 3 in the Erythrocyte Membrane Structural Changes Under Isotonic and Hypotonic Conditions

Ivana Pajic-Lijakovic and Milan Milivojevic

Additional information is available at the end of the chapter

http://dx.doi.org/10.5772/64964

Abstract

An attempt was made to discuss and connect various modeling approaches which have been proposed in the literature in order to shed further light on the erythrocyte membrane relaxation under isotonic and hypotonic conditions. Roles of the main membrane constituents: (1) the actin-spectrin cortex, (2) the lipid bilayer, and (3) the transmembrane protein band 3 and its course-consequence relations were considered to estimate the membrane relaxation phenomena. Cell response to loading conditions includes the successive sub-bioprocesses: (1) erythrocyte local or global deformation, (2) the cortex-bilayer coupling, and (3) the rearrangements of band 3. The results indicate that the membrane structural changes include: (1) the spectrin flexibility distribution and (2) the rate of its changes influenced by the number of band 3 molecules attached to spectrin filaments, and phosphorylation of the actin-spectrin junctions. Band 3 rearrangement also influences: (1) the effective bending modulus and (2) the band 3-bilayer interaction energy and on that base the bilayer bending state. The erythrocyte swelling under hypotonic conditions influences the bilayer integrity which leads to the hemolytic hole formation. The hemolytic hole represents the excited cluster of band 3 molecules.

Keywords: packing state changes of band 3 clusters, reversible hemolytic hole formation, the lipid bilayer bending state changes, the spectrin inter- and intrachain interactions, mathematical modeling

1. Introduction

Erythrocyte mechanics under isotonic and hypotonic conditions has been studied from engineering and biomedical stand points [1–14]. Rheological response of the erythrocyte

membrane depends on the main membrane constituent rearrangement: (1) the actin cortex, (2) the lipid bilayer, and (3) the transmembrane protein band 3. The membrane fluctuations under isotonic condition induce alternating expansion and compression of the membrane parts in order to ensure surface and volume conservation. The membrane relaxation occurs within (millisecond order) affine regime and (second order) nonaffine regime. The affine regime corresponds to the spectrin interchain interactions while the nonaffine regime corresponds to the spectrin intrachain interactions. However, the membrane fluctuations under hypotonic condition induce volume increase by ensuring surface conservation. The membrane response under hypotonic condition includes the successive sub-processes: (1) erythrocyte swelling, (2) lifetime of the lipid structural integrity and the rearrangement of transmembrane protein band 3, and (3) the reversible hemolytic hole formation and hemoglobin (Hb) release to surrounding solution. Duration of the membrane relaxation depends on contributions of three subprocesses: (1) time for cell swelling $t_{sw} \in [5, 100\ s]$, (2) membrane lifetime $\tau_m \in (0,\ t_H)$ (where t_H is the hemolytic time), and (3) time for Hb release from already formed hemolytic hole during successive open-closed state changes $t_{release} \in [1{,}5\ s]$ [11, 13].

The band 3 rearrangement significantly influences the state of both, the lipid bilayer and the actin-spectrin cortex. Space distribution of band 3 molecules and their lateral diffusion influence the bending state of the lipid bilayer and its free energy [15–17]. Local changes of the bilayer bending state enhance anomalous sub-diffusion and eventually lead to hop-diffusion of lipids. These effects induce anomalous nature of energy dissipation during lipids structural ordering and could be quantified by the effective viscosity [18]. The bilayer structural changes have the feedback effects to band 3 protein-lipids positive hydrophobic mismatch effects [19–21]. De Meyer et al. [19] pointed to the cholesterol role in lipid mediated protein-protein interactions. These effects could lead to the protein tilt angle changes and the protein clustering. This clustering can be modulated by homotypic interactions of the protein transmembrane domains and electrostatic protein-lipid interactions [21]. Tilt angle changes influence packing state of band 3 clusters and their association-dissociation to spectrin. Band 3 molecules form various complexes with spectrin and influence its conformational changes. In-homogeneous distribution of band 3 molecules and their ability to clustering influence the rheological response of: (1) the bilayer, (2) the cortex, and (3) the nature of the bilayer-cortex mechanical coupling. Ehrig et al. [22] pointed that the lipid bilayer phase separation can be strongly affected by interaction with the actin cortex, which, depending on the temperature and membrane composition, can either lead to precipitation of highly dynamic membrane domains (rafts), or prevent large-scale phase separation.

For understanding the influence of band 3 rearrangement on complex nature of the membrane rheological response, it is necessary to consider three subpopulations of band 3 molecules under isotonic and hypotonic conditions. The first subpopulation (20–40%) as tetramers forms high affinity complexes with ankyrin (quantified by the dissociation constant ~5 nM) as reported by Tomishige et al. [23] and Kodippili et al. [24]. Band 3-ankyrin complexes are located near the center of spectrin tetramers. These complexes could survive the hypotonic conditions. Golan and Veatch [25] reported that 25% of band 3 population

http://dx.doi.org/10.5772/64964

remains attached to the cortex under ionic strength 26 mM $NaPO_4$ solution at 37°C. The second subpopulation (~30%) as dimers forms lower affinity complexes with the adducin (the dissociation constant is ~100 nM) as reported by Franco and Low [26] and Kodippili et al. [24]. This subpopulation is located at the spectrin-actin junction complexes. The junctions of the network link 4–7 spectrin filaments [27]. The third one is freely diffusing subpopulation (~30%). The part of freely diffusing subpopulation increases under hypotonic conditions. Golen and Veatch [25] determined that mobile fraction of band 3 molecules under the external solution tonicity 46.0 mM $NaPO_4$ at 21°C was 11 ± 9%. Under tonicity of 5.2 mM $NaPO_4$ at 21°C, the mobile fraction of band 3 molecules was 72 ± 7%. Band 3 molecules are anion at pH = 7. The value of Stokes radius of band 3 dimmer is approximately 7.6 nm while for tetramer is 11 nm at room temperature and pH = 7.2 [28]. The total number of band 3 per single erythrocyte is $\sim 1 \times 10^6$. Thermal fluctuations of the erythrocyte membrane could induce conformational changes of cytoplasmic domain of transmembrane protein band 3 [29]. Such conformational changes result in electrostatic interactions between highly anionic N-terminal domains of band 3 molecules and on that base intensified their short-range self-associative tendency [28]. Long-range self-associative tendency is induced by positive hydrophobic mismatch effects [21]. The band 3 clustering is pronounced under hypotonic conditions [30]. In this case, ~25% of band 3 molecules make aggregate of ~5000 mers [31]. All band 3 subpopulations through these complexes contribute to the spectrin conformational changes by reducing its mobility and influence the cortex stiffening.

The band 3 molecules within the freely diffusing subpopulation could form low affinity complexes to spectrin (the dissociation constant is ~1–10 μM) [25]. On that base, they influence spectrin conformations [32]. Gov [32] reported that the parts of the spectrin filament between two mid-point attachments behave as independent blobs. The main factor which influences the spectrin flexibility and conformations is $\frac{l}{L_p}$ (where l is the length of the filament part between two mid-point attachments and L_p is the spectrin persistence length $L_p = 15-25\ nm$ [33]). The spectrin filament parts are as follows: (1) flexible if $\frac{l}{L_p} \succ\succ 1$, (2) semiflexible if $\frac{l}{L_p} \approx 1$, and (3) rod-like if $\frac{l}{L_p} \prec\prec 1$. The average length of spectrin parts is equal to $\langle l \rangle = \frac{L_c}{\langle N_B \rangle}$ (where $L_c \approx 200$nm is the spectrin contour length [27] and $\langle N_B \rangle \approx 4-10$ is the average number of attached band 3 molecules per single spectrin filament [34]). The length of the spectrin parts depends on the rearrangement of band 3 molecules which include their lateral diffusion and self-associative tendency [28]. Consequently, rheological behavior of the cortex is related to the spectrin flexibility distribution and the rate of its changes [35, 36]. Deeper insight into coarse-consequence relations between the band 3 rearrangement and the spectrin inter- and intrachain interactions as well as the bilayer bending offers a possibility for understanding the complex nature of the membrane relaxation phenomena.

2. Rearrangement of band 3 molecules-cluster packing state changes

Packing state of band 3 clusters and its changes during short-time lateral motion under isotonic and hypotonic conditions could be estimated by applying Edwards' statistics [30, 35, 37, 38]. Short-time motion of band 3 molecules includes: (1) Brownian diffusion within the mesh compartment of the spectrin-actin cortex and (2) hop diffusion between two compartments. Hop is observed at every 350 ms [23]. Band 3 molecules form clusters caused by positive hydrophobic mismatch effects during their lateral diffusion. This statistical approach is suitable for describing the cluster packing state changes under vibration field. Edwards introduced a new and very significant parameter for description of particle clusters named compactivity of the cluster part X representing the change of cluster part volume V_{cr} with entropy S_{cr} for given number of molecules N_p (i.e., considering it as a canonical ensemble):

$$X = \left(\frac{\partial V_{cr}}{\partial S_{cr}} \right)_{N_P} \tag{1}$$

The two limits of the compactivity have been introduced: (1) $X \to 0$ corresponds to the most compact particle rearrangement and (2) $X \to \infty$ corresponds to the least compact particle rearrangement. When $X \to 0$, the system picks out one particular configuration as being most likely, and when $X \to \infty$, the system picks out all configurations as being equally likely. Probability distribution of band 3 cluster states could be expressed as:

$$P = e^{(Y_r - W_r)/\lambda X} \tag{2}$$

where Y_r is effective volume of the cluster part (corresponding to the free energy F in classical statistical mechanics) and W_r is the "volume function" corresponding to the Hamiltonian and λ is constant adjusting dimensions. Then, we can write:

$$Y_r = V_{cr} + X \frac{\partial Y_r}{\partial X} = V_{cr} - XS_{cr} \tag{3}$$

Cluster is considered as canonical ensemble during short-time rearrangement. The partition function relating Y_r with the volume function of a cluster part $W_r(q)$ can be written in the form:

$$Z_p = e^{-\frac{Y_r}{\lambda X}} = \int\int \ldots \int \Omega_w e^{-\frac{W_r(q_1, q_2, \ldots q_n)}{\lambda X}} dq_1 dq_2 \ldots dq_n \tag{4}$$

http://dx.doi.org/10.5772/64964

where integration goes over all geometrical degrees of freedom (DOFs) q_i of all molecules in the cluster, $Z_p = Z_p(r, t_{eq})$ is the partition function. The key step is the identification of an exact volume function which makes it possible to pinpoint the configuration phase space and evaluate its dimensionality. We consider weakly interacting systems. To be precise, the interactions must be sufficient to lead to thermodynamical equilibrium, but weak enough that these interactions have negligible effects on the effective volume of individual molecules.

$$W_r(n_q) = N_{pr} w_p(q_1, q_2, \ldots, q_n) \tag{5}$$

where $w_p(q_1, q_2, \ldots, q_n)$ is the volume function of single molecule. Rearrangement of rigid molecules such as band 3 within the cluster could be described using low degrees of freedom (DOFs). For this case, the DOFs describe molecule's orientation in the cluster part located at r and its coordination number.

The band 3 cluster excitation under isotonic condition induces the molecule orientation changes presented in **Figure 1**. The excitation occurs during alternating expansion and compression of the membrane parts in order to ensure surface and volume conservation.

The corresponding volume function could be expressed as [30, 35]:

$$w_p(q_o, q_c) = v_0 + \Delta v_o q_o^2 \tag{6}$$

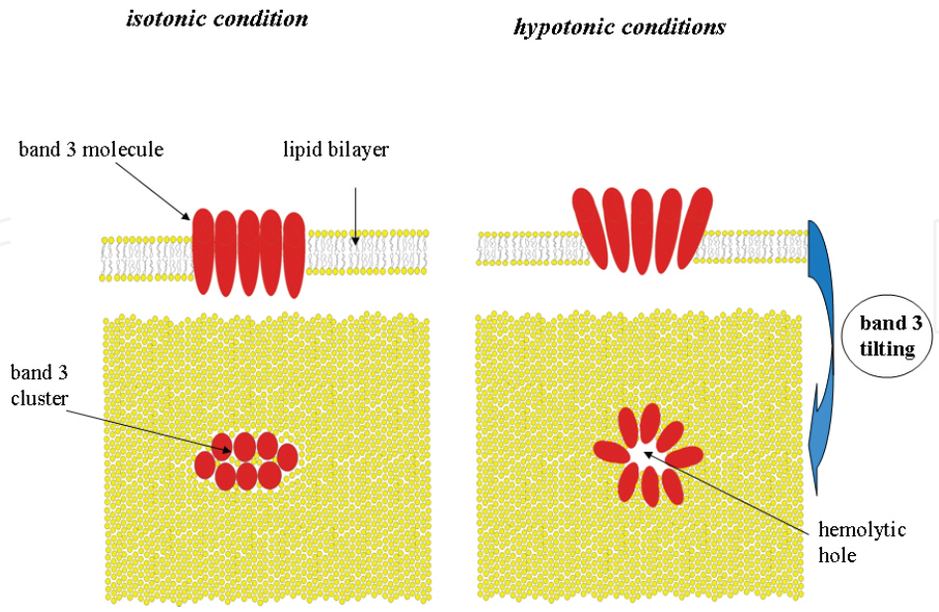

Figure 1. Schematic representation of the packing state changes for excited band 3 cluster under isotonic and hypotonic conditions.

where v_0 is the minimum specific volume of single molecule of band 3 $v_0 = \frac{4}{3}\langle r_s \rangle_{\min}^3 \pi$, $\langle r_s \rangle_{\min}$ is the minimum of the molecule Stokes radius, Δv_o is the volume increment caused by the molecule orientation equal to $\Delta v_o = v_{\max} - v_0$, $v_{\max}$ is the maximum specific volume of single molecule of band 3 $v_{\max} = \frac{4}{3}\langle r_s \rangle_{\max}^3 \pi$, $\langle r_s \rangle_{\max}$ is the maximum of the molecule Stokes radius, q_o accounts the molecule's orientation equal to $q_o^2 = \frac{1}{2}\sum_i q_{oi}^2$ while q_{oi} accounts various directions, Δv_o is the volume increment contributions caused by the DOFs q_o changes. For molecule loose packing, we can take $w_p = v_0 + \Delta v_o$ and a molecule has high values of the degrees of freedom in such system so q_i values are close to 1.

The band 3 cluster excitation under hypotonic conditions is more intensive than that obtained under isotonic condition due to changes the bilayer bending state during erythrocyte swelling. The excitation could induce changes the packing state from close packing to ring-like structure which represents the reversible hemolytic hole. These changes are influenced by the positive hydrophobic mismatch effects which could induce protein tilting [20]. Zade-Oppen [13] reported that the average hole opening time period is 270 ms, while the average hole closing time period is 260 ms. Seeman et al. [8] experimentally determined the diameter of the reversible osmotic holes in the range between 10 and 100 nm for human erythrocyte under hypotonic condition at pH = 7. Accordingly, the smaller hemolytic hole corresponds to ~4 band 3 molecules while the larger one corresponds to ~40 molecules [18, 30]. The result points out that cluster size is not the main factor for the hole formation. The main factor could be the hydrophobic mismatch effects between band 3 and the surrounding lipid bilayer as was shown in **Figure 1**. The corresponding volume function is as follows:

$$w_p(q_o, q_c) = v_0 + \Delta v_o q_o^2 + \Delta v_c q_c^2 \tag{7}$$

where q_c accounts the coordination number, Δv_c is the volume increment caused by changes the molecule coordination number equal to $\Delta v_c = \frac{R_H^2(t_R)\ \pi\ h_m}{N_r(t_R)}$, t_R is the relaxation time, h_m is the thickness of the lipid bilayer for already swollen erythrocyte, $R_H(t_R)$ is the radius of hemolytic hole, $N_r(t_R)$ is the number of molecules per cluster located at r. DOFs can have values in the range 0 to 1. When $q_c = 0$ and $q_{oi} = 0$ at $t_R \to t_{R\,eq}$, the volume function is $w_p = v_0$. When $q_c = 1$ and $q_{oi} = 1$ at $t_R = 0$, the volume function is equal to $w_p = v_0 + \Delta v_o + \Delta v_c$. This excited cluster state represents the hemolytic hole.

Band 3 molecules change their states during migration. Consequently, for estimating the DOFs temporal changes it is necessary to consider the temporal changes of single molecule velocity.

http://dx.doi.org/10.5772/64964

Temporal changes of DOFs under vibration field could be described in the form of Langevin-type equations [30, 37]:

$$\frac{dq_i(t_R)}{dt_R} = -\frac{1}{\gamma_q}\frac{\partial w_p\left(q_i(t_R)\right)}{\partial q_i(t_R)} + \phi_q(t_R) \tag{8}$$

where the stochastic random force $\phi_q(t_R)$ is formulated as white noise with correlation function $\langle\phi_q(t_R)\phi_q(t_R')\rangle = 2\lambda X\gamma_q\delta_{ij}\delta(t_R - t_R')$, and γ_q is the analog of frictional resistance. System structural changes could induce anomalous nature of energy dissipation derivative during molecules migration within the cluster. If the molecule migration causes damping effects as described by Tomishige et al. [23] (subdiffusion phenomenon), the derivative $\frac{dq_i(t_R)}{dt_R}$ could be replaced by the fractional derivative D_t^γ (where D_t^γ is the Caputo's fractional derivative, γ is the order of the fractional derivative such that $\gamma \prec 1$). Caputo's definition of the fractional derivative of some function $f(t)$ is given as follows [39]: $D_t^\gamma(f(t)) = \frac{1}{\Gamma(1-\gamma)}\frac{d}{dt}\int_0^t \frac{f(t')^{(1)}}{(t-t')^\gamma}dt'$ (where $\Gamma(1-\gamma)$ is the gamma function). Average equilibrium volume of single molecule is obtained as:

$$v_{p\ eq} = \frac{\iint\cdots\int w_{pr}(\bullet)\ e^{-\frac{w_{pr}(\bullet)}{\lambda X}}\ d[\bullet]}{Z_p} \tag{9}$$

where $Z_p(r, t_{Req})$ is the partition function, and $V_{cr}\left(r, t_{Req}\right) = N_p\left(r, t_{Req}\right)\ v_{p\ eq}$ is the cluster volume.

3. Band 3 rearrangement influences the spectrin inter- and intrachain interactions and the bilayer bending

The spectrin interchain interactions depend on the number of band 3 molecules attached per single spectrin filament as was shown in **Figure 2**.

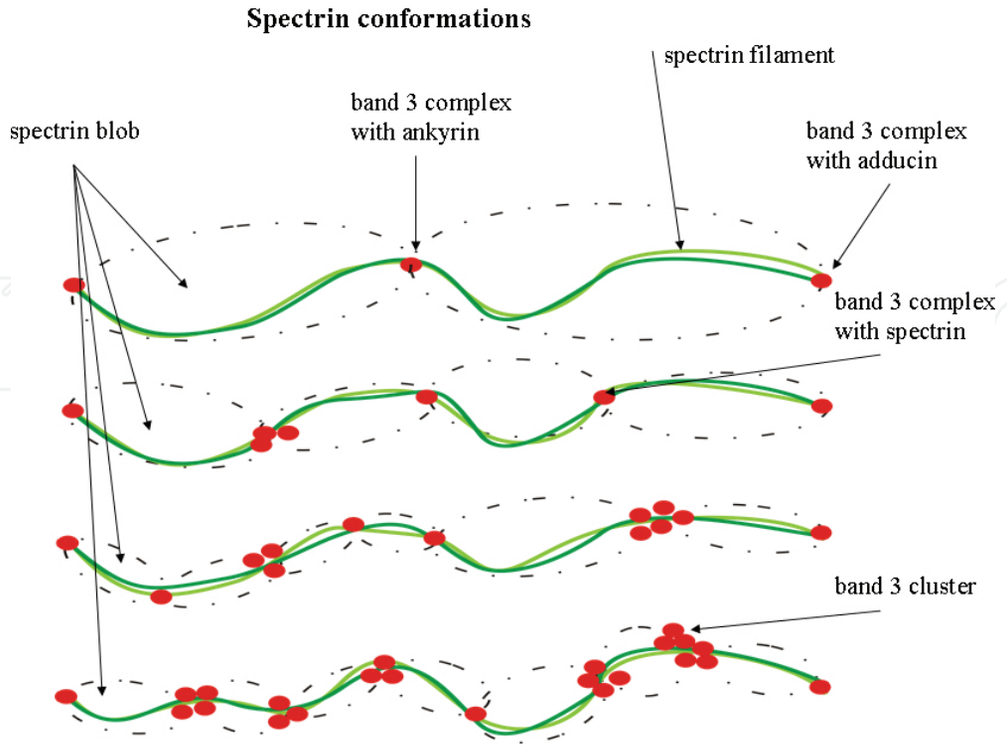

Figure 2. Spectrin conformational changes influenced by the number of attached band 3 molecules.

The spectrin filaments have been treated as flexible ($\frac{L_c}{L_p} \succ \succ 1$) [27] and semiflexible ($\frac{L_c}{L_p} \approx 1$) [40] (where L_c is the spectrin contour length equal to $L_c = \sum_{i=1}^{N_B-1} l_i$, l_i is the length of i-th filament part between two mid-point attachments of band 3). The flexibility depends on the number of band 3 molecules attached per single spectrin filament. Spectrin filament without band 3-spectrin complexes behaves as flexible. Its conformations have been described as [27]:

$$F_s \approx N\mu_s \left(R - \left\langle r_g^2 \right\rangle^{1/2} \right) \tag{10}$$

Where $N \approx 3$ is the number of spectrin filaments per network units, μ_s is the surface shear modulus of the cortex equal to $\mu_s = \frac{k_B T}{\langle r_g^2 \rangle}$, k_B is Boltzmann constant and T is temperature, R is the end-to-end distance of spectrin filaments in the cortex, $\langle r_g^2 \rangle^{1/2}$ is the average filaments radius of gyration. If the band 3-spectrin low affinity complexes exist, the parts of the spectrin filament between the complexes behave as independent blobs [32]. The conformation changes within the blobs are the milliseconds order [32]. When $\frac{\langle l \rangle}{L_p} \succ \succ 1$ the filament parts are flexible, but if $\frac{\langle l \rangle}{L_p} \approx 1$ they become semiflexible, while if $\frac{\langle l \rangle}{L_p} \prec \prec 1$ they behave as rod-like polymers (where $\langle l \rangle$

http://dx.doi.org/10.5772/64964

is the average length of the filament part) [41]. Li et al. [40] treated the whole spectrin filaments as a semiflexible and proposed worm-like force for modeling of the spectrin conformations:

$$F_{wlc} = \frac{k_B T}{L_p}\left\{\frac{1}{4\left(1-x\right)^2} - \frac{1}{4} + x\right\} \tag{11}$$

where $x = \frac{R - \left\langle r_g^2 \right\rangle^{1/2}}{L_c}$ is the stretch ratio. The worm-like force corresponds to the condition $\frac{L_c}{L_p} \approx 1$ [41]. It is in accordance with the fact that the spectrin-band 3 complexes lead to decrease in the spectrin flexibility. It could be quantified by apparent increase in the spectrin persistence length $L_p \rightarrow L_{p\,eff}$ (where $L_{p\,eff}$ is the effective spectrin persistence length). The concept of effective persistence length has been introduced for describing the nature of interchain structural changes for worm-like chains such as proteins under stretching [42, 43]. On that base, the effective persistence length in our case could be expressed as [36]:

$$L_{p\,eff}\left(T, N_B\right) = L_p\left(T\right) + \Delta L_p\left(N_B\right) \tag{12}$$

Where $L_{p\,eff}(T,\ N_B)$ is the effective persistence length of spectrin filament, $L_p(T)$ is the spectrin persistence length for the filaments without mid-point attachments at the same temperature conditions and $\Delta L_p(N_B)$ is the contribution to the persistence length caused by the band 3 midpoint attachments. The collective phenomena among variously flexible spectrin filaments induce generation of the cortex in-homogeneities [36]. The in-homogeneities in the context of the cortex micro domains influence the cortex relaxation. The cortex relaxation modulus $G_C(t_R)$ could be expressed as [18, 36]:

$$G_C\left(t_R\right) = \int_{L_{p\min}}^{L_{p\max}} \rho_C\left(L_{p\,eff}, t_R\right)\ G_C\left(L_{p\,eff}, t_R\right)\ dL_{p\,eff} \tag{13}$$

where $G_C(L_{p\,eff},\ t_R)$ is the cortex relaxation modulus within the domain and $\rho_C(L_{p\,eff},\ t_R)$ is the spectrin flexibility distribution caused by the band 3 rearrangement.

The presence of the cortex micro domains is related to in-homogeneous distribution of: (1) band 3 molecules, (2) spectrin flexibility, and (3) the presence of the cortex defects as was shown in **Figure 3**. Cumulative effects as: (1) the spectrin intrachain interactions which lead to formation of the cortex micro domains, (2) longtime diffusion of band 3 molecules, and (3) longtime bending relaxation of the lipid bilayer are at the order of seconds [18].

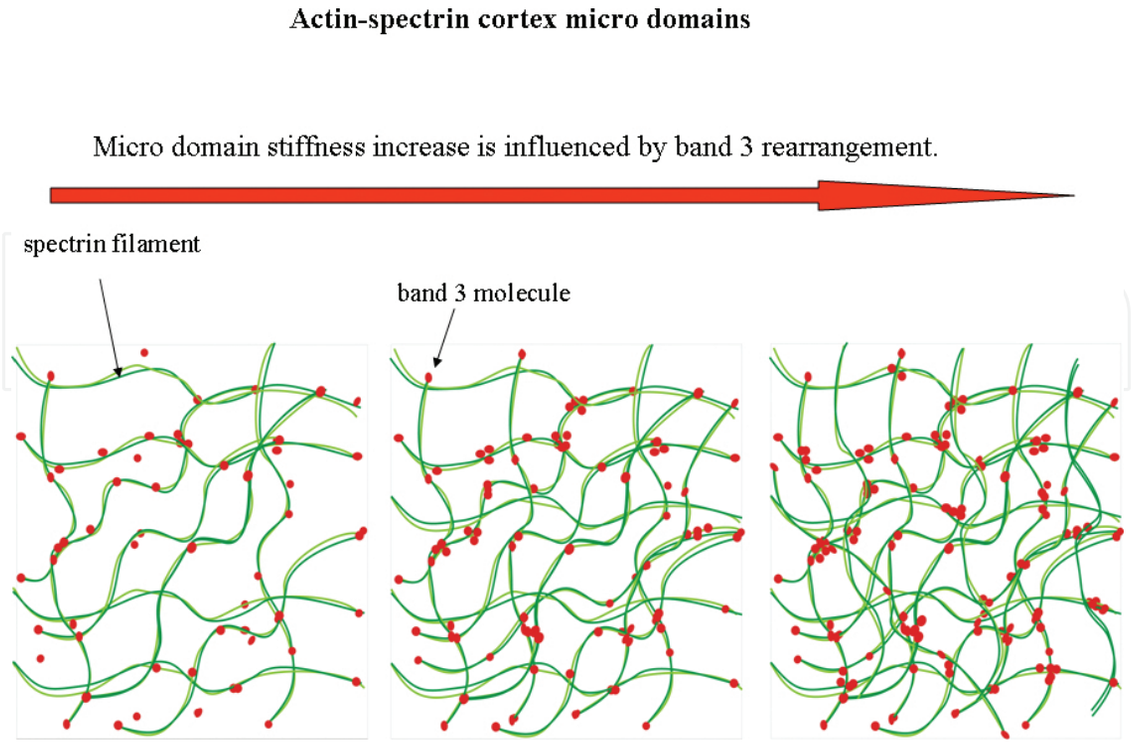

Figure 3. The cortex micro domains—schematic representation.

These local in-homogeneities of the cortex are caused by alternating expansion and compression of the membrane and the cortex-bilayer coupling. The bilayer bending is influenced by conformational changes of the two types of spectrin filaments [44]: (1) type 1—corresponds to the filaments grafted at one end or at both ends but not connected to the stretched cortex and (2) type 2—corresponds to the filaments grafted at both ends and on that base represents a part of the connected stretched cortex. Filaments within the type 1 induce a concave curvature of radius $R_{L\ 1}$, while the type 2 induce a concave curvature of radius $R_{L\ 2}$ such that $R_{L\ 1} = -R_{L\ 2}$. The bilayer-cortex coupling has been expressed by Helfrich-type bending-free energy functional [44]:

$$E(n_1, n_2) = \frac{1}{2}\kappa w \int \left(H - \bar{H}_1 n_1(r,s,t_R) - \bar{H}_2 n_2(r,s,t_R)\right)^2 d^2 s \tag{14}$$

Where s is the coordinate along the contour, κ is the bending modulus of the bilayer, w is the bilayer width, $n_1(r, s, t_R)$ and $n_2(r, s, t_R)$ are the relative densities of the types 1 and 2 of spectrin filaments, and the corresponding local mean curvature are $\overline{H}_1 = \frac{1}{R_{L\ 1}}$ and $\overline{H}_2 = \frac{1}{R_{L\ 2}}$. The overall curvature by spectrin filaments is expressed as $\overline{H}_1 n_1 + \overline{H}_2 n_2$. Band 3 molecules influence the lipid bilayer bending modulus. Shlomovitz and Gov [45] formulated the apparent bending modulus equal to:

http://dx.doi.org/10.5772/64964

$$\kappa_{app}(\varphi) = \kappa\left(1-\varphi\left(r,t_R\right)\right)+\kappa'\varphi\left(r,t_R\right) \tag{15}$$

where $\kappa_{app}(\varphi)$ is the apparent bending modulus, κ is the bending modulus of the bilayer without band 3 molecules, κ' is the contribution of band 3 molecules to the bending modulus, $\varphi(r, t)$ is the local surface fraction of the band 3 molecules. Shlomovitz and Gov [45] expressed the influence of inclusions (band 3 molecules) on the lipid bilayer bending by formulating the free energy functional as:

$$E(\varphi) = \int \frac{1}{2}\kappa_{app}(\varphi)\left(H-\varphi\bar{H}\right)^2 d^2r \tag{16}$$

Consequently, the model Eqs. (15) and (16) could be combined to describe the influence of: (1) spectrin conformationals and (2) band 3 molecules migration on the lipid bilayer bending state expressed in the form: $E(n_1, n_2, \varphi) = \int \frac{1}{2}\kappa_{app}(\varphi)\, w \int \left(H-(1-\varphi)\left(\bar{H}_1 n_1 + \bar{H}_2 n_2\right)\right)^2 d^2 s\, d^2 r$.
The collective phenomena related to the spectrin filaments migration is expressed by spatial-temporal changes of the conservative variable $n = n(r, s, t_R)$ [46] as:

$$\frac{1}{\dot{s}}\frac{\partial(\dot{s}\, n)}{\partial t_R} = \frac{D}{\dot{s}}\nabla_s^2(\dot{s}\, n) + \frac{1}{\dot{s}}\frac{\Lambda}{n_{sat}}\nabla_s\left(\dot{s}\, n\nabla_s\left(\frac{1}{\dot{s}}\frac{\delta E}{\delta n}\right)\right) \tag{17}$$

where $D = \frac{k_B T}{\Lambda}$ is the spectrin collective diffusion coefficient which accounted for the intrachain interactions, Λ is the filaments mobility parameter, n_{sat} is the maximal packing density of the filaments, and ∇_s is the derivative along the contour s. Spectrin filament mobility depends on the number of attached band 3 molecules. Consequently, the effective diffusivity could be formulated as $D_{eff} = D_{eff}(\varphi)$and introduced in eq. 17. Shlomovitz and Gov [45] modeled the collective migration of band 3 molecules as:

$$\frac{\partial\varphi}{\partial t_R} = D_B\nabla^2\varphi + \Lambda_B\nabla\left(\varphi\nabla\left(\frac{\delta E}{\delta\varphi}\right)\right) \tag{18}$$

where ∇ is the derivative along the space, Λ_B is the band 3 lateral mobility and D_B is the band 3 diffusion coefficient equal to $D_B = \frac{k_B T}{\Lambda_B}$. Lateral motion of the band 3 molecules induces the anomalous nature of energy dissipation which includes damping effects [23]. These damping effects are induced from band 3 association-dissociation to spectrin filaments. Pajic-Lijakovic [35, 36] proposed fractional Langevin equation for describing the lateral diffusion by applying

the fractional derivatives [39]. Consequently, the time derivatives from Eqs. (17) to (18) could be replaced by the fractional derivative $D_t^{\alpha}(\bullet)$.

4. Conclusion

Rheological behavior of the cortex depends on the spectrin flexibility distribution and the rate of its changes [35, 36]. The spectrin flexibility primarily depends on the number of band 3 molecules attached per single spectrin filaments. Rearrangement of the band 3 molecules and their lateral diffusion also influence the bending modulus of the lipid bilayer and the band 3-bilayer interaction energy. Consequently, the band 3 rearrangement influences the cortex-bilayer coupling and on that base influences the membrane rheological behavior as a whole. The membrane structural changes induce anomalous nature of energy dissipation caused by these complex multi scale molecular dynamics.

Acknowledgements

This research was funded by grant III46001 from the Ministry of Science and Environmental Protection, Republic of Serbia.

Author details

Ivana Pajic-Lijakovic* and Milan Milivojevic

*Address all correspondence to: iva@tmf.bg.ac.rs

Faculty of Technology and Metallurgy, Belgrade University, Belgrade, Serbia

References

[1] Amin MS, Park YK, Lue N, Dasari RR, Badizadegan K, Feld MS, Popescu G. Micro-rheology of red blood cell membrane using dynamics scattering microscopy. Opt Express. 2007; 15(25):17001–17009.

[2] Popescu G, Park YK, Dasari RR, Badizadegan K, Feld MS. Coherence Properties of red blood cell membrane motion. Phys Rev E. 2007; 76:031902 1–5.

[3] Puig-de-Morales-Marinkovic M, Turner KT, Butler JP, Fredberg JJ, Suresh S. Viscoelasticity of the human red blood cell. Am J Physiol Cell Physiol. 2007; 293:C597–C605.

[4] Yoon YZ, Kotar J, Yoon G, Cicuta P. The nonlinear mechanical response of the red blood cell. Phys Biol. 2008; 5(3):036007 1–8.

[5] Yoon YZ, Kotar J, Brown AT, Cicuta P. Red blood cell dynamics: from spontaneous fluctuations to non-linear response. Soft Matter. 2011; 7:2042–2051.

[6] Park YK, Best CA, Badizadegan K, Dasari RR, Feld MS, Kuriabova T, Henle ML, Levine AJ, Gabriel Popescu G. Measurement of red blood cell mechanics during morphological changes. PNAS. 2010; 107(15):6731–6736.

[7] Danon D. Osmotic hemolysis by a gradual decrease in the ionic strength of the surrounding medium. J Cell Comp Physiol. 1961; 57:111–117.

[8] Seeman P, Cheng D, Iles GH. Structure of membrane holes in osmotic and saponian hemolysis. J Cell Biol. 1973; 56:519–527.

[9] Leiber MR, Steck TL. A description of the holes in human erythrocyte membrane ghosts. J Biol Chem. 1982; 257:11651–11659.

[10] Sato Y, Yamakose H, Suzuki Y. Mechanism of hypotonic hemolysis of human erythrocytes. Biol Pharm Bull. 1993; 16(5):506–512.

[11] Pribush A, Meyerstein D, Meyerstein N. Kinetic of erythrocyte swelling and membrane hole formation in hypotonic media. Bioch Biophys Acta. 2002; 1558:119–132.

[12] Evans EA, Hochmuth RM. Membrane viscoelasticity. Biophys J. 1976; 16:1–11.

[13] Zade-Oppen AMM. Repetitive cell 'jump' during hypotonic lysis of erythrocytes observed with simple flow chamber. J Microsc. 1998; 192:54–62.

[14] Markle DR, Evans EA, Hochmuth RM. Force relaxation and permanent deformation of erythrocyte membrane. Biophys J. 1983; 42:91–98.

[15] Gil T, Ipsen JH, Mouritsen OG, Sabra MC, Sperotto MM, Zuckermann MJ. Theoretical analysis of protein organization in lipid membranes. Biochem Biophys Acta. 1998; 1376:245–266.

[16] Evans AR, Turner MS, Sens P. 2003. Interactions between proteins bound to biomembranes. Phys Rev E. 2003; 67:041907 1–10.

[17] Sens P, Turner MS. Theoretical model for the formation of caveolae and similar membrane invaginations. Biophys J. 2004; 86:2049–2057.

[18] Pajic-Lijakovic I, Milivojevic M. Modeling analysis of the lipid bilayer-cytoskeleton coupling in erythrocyte membrane. Biomech Model Mechanobiol. 2014; 13(5):1097–1104.

[19] De Meyer FJM, Rodgers JM, Willems TF, Smit B. Molecular simulation of the effect of cholesterol on lipid-mediated protein-protein interactions. Biophys J. 2010; 99:3629–3638.

[20] Strandberg E, Esteban-Martin S, Ulrich AS, Salgado J. Hydrophobic mismatch of mobile transmembrane helices: merging theory and experiments. Biochim Biophys Acta. 2012; 1818:1242–1249.

[21] Milovanovic D, Honigmann A, Koike S, Gottfert F, Pahler G, Junius M, Muller S, Diederichsen U, Janshoff A, Grubmuller H, Risselada HJ, Eggeling C, Hell SW, van den Bogaart G, Jahn R. Hydrophobic mismatch sorts SNARE proteins into distinct membrane domains. Nature Commun. 2015; 6:5984 1–10.

[22] Ehrig J, Petrov EP, Schwille P. Near-critical fluctuations and cytoskeleton-assisted phase separation lead to sub diffusion in cell membranes. Biophys J. 2011; 100:80–89.

[23] Tomishige M, Sako Y, Kusumi A. Regulation mechanism of the lateral diffusion of band 3 in erythrocyte membranes by the membrane skeleton. J Cell Biol. 1998; 142(4):989–1000.

[24] Kodippili GC, Spector J, Hale J, Giger K, Hughes MR, McNagny KM, Birkenmeier C, Peters L, Ritchie K, Low PS. Analysis of the mobilities of band 3 populations asociatted with ankyrin protein and junctional complexes in intact murine erythrocytes. J Biol Chem. 2012; 287(6):4129–4138.

[25] Golan DE, Veatch W. Lateral mobility of band 3 in the human erythrocyte membrane studied by fluorescence photobleaching recovery: evidence for control by cytoskeletal interactions, PNAS. 1980; 77(5):2537–2541.

[26] Franco T, Low PS. Erythrocyte adducin: a structural regulator of the red blood cell membrane. Transfus Clin Biol. 2010; 17(3):87–94.

[27] Gov NS, Safran SA. Red blood cell membrane fluctuations and shape controlled by ATP-induced cytoskeletal defects. Biophys J. 2005; 88:1859–1874.

[28] Taylor AM, Boulter J, Harding SE, Colfen H, Watts A. Hydrodynamics properties of hyman erythrocyte band 3 solubilized in reduced triton X-100. Biophys J. 1999; 76:2043–2055.

[29] Salhany JM, Cordes KA, Sloan RL. Mechanism of band 3 dimmer dissociation during incubation of erythrocyte membranes at 37 degrees C. Biochem J. 2000; 345:33–41.

[30] Pajic-Lijakovic I, Ilic V, Bugarski B, Plavsic MB. The rearrangement of erythrocyte band 3 molecules and reversible osmotic holes formation under hypotonic conditions. Europ Biophys J Biophys Lett. 2010; 39(5):789–800.

[31] Blackman SM, Cobb CE, Beth AH, Piston DW. The orientation of eosin-5-maleimide on human erythrocyte band 3 measured by fluorescence polarization microscopy. Biophys J. 1996; 71:194–208.

[32] Gov NS. Less is more: removing membrane attachments stiffness the RBC cytoskeleton. New J Phys. 2007; 9:430 1–14.

[33] Boal D. Mechanics of the Cell. 2nd edition. New York: Cambridge University Press, 2012.

[34] Waugh RE, Agre P. Reductions of erythrocyte membrane viscoelastic coefficients reflect spectrin deficiencies in hereditary spherocytosis. J Clin Invest. 1988; 81:133–141.

[35] Pajic-Lijakovic I. Erythrocytes under osmotic stress–modeling considerations. Progr Biophys Mol Biol. 2015; 117(1):113–124.

[36] Pajic-Lijakovic I. Role of band 3 in erythrocyte membrane structural changes under thermal fluctuations-modeling considerations. J Bioen Biomem. 2015; 47(6):507–518.

[37] Edwards S, Grinev DV. Statistical mechanics of vibration-induced compaction of powders. Phys Rev E. 1988; 58(4):4758–4762.

[38] Edwards SF. The full canonical ensemble of a granular system. Phys A. 2005; 353:114–118.

[39] Podlubny I. Fractional Differential Equations, Mathematics in Science and Engineering. London: Academic Press, 1999, 198, 78.

[40] Li J, Dao M, Lim CT, Suresh S. Spectrin-level modeling of the cytoskeleton and optical tweezers stretching of the erythrocyte. Biophys J. 2005; 88:3707–3719.

[41] Pritchard RH, Huang YYS, Terentjev EM. Mechanics of biological networks: from the cell cytoskeleton to connective tissue. Soft Matter. 2014; 10:1864–1884.

[42] Bouchiat C, Wang MD, Allemand JF, Strick T, Block SM, Croquette V. Estimating the persistence length of a worm-like chain molecule from force-extension measurements. Biophys J. 1999; 76:409–413.

[43] Nir G, Lindner M, Dietrich HRC, Girshevitz O, Vorgias CE, Garini Y. HU protein induces incoherent DNA persistence length. Biophys J. 2011; 100:784–790.

[44] Kabaso D, Shlomovitz R, Auth T, Lew VL, Gov NS. Curling and local shape changes of red blood cell membranes driven by cytoskeletal reorganization. Biophys J. 2010; 99:808–816.

[45] Shlomovitz R, Gov NS. Curved inclusions surf membrane waves. Europhys Lett. 2008; 84:58008 1–6.

[46] Kabaso D, Shlomovitz R, Auth T, Lew VL, Gov NS. Cytoskeletal Reorganization of Red Blood Cell Shape: Curling of Free Edges and Malaria Merozoites. In: Iglic A, editor. Advances in Planar Lipid Bilayers and Liposomes, Volume 13; Amsterdam: Elsevier, 2011. p. 73–102.

IntechOpen